Respiratory Physiology & Neurobiology 269 (2019) 103250

Contents lists available at ScienceDirect

Respiratory Physiology & Neurobiology

journal homepage: www.elsevier.com/locate/resphysiol

Acute lung injury in neonatal rats causes postsynaptic depression in nucleus tractus solitarii second-order neurons

Paulina M. Getsy[a,c], Catherine A. Mayer[c], Peter M. MacFarlane[c], Frank J. Jacono[b,e], Christopher G. Wilson[d,*]

[a] Department of Physiology and Biophysics, CWRU School of Medicine, Cleveland, OH, 44106, United States
[b] Division of Pulmonary, Critical Care and Sleep Medicine, Department of Medicine, CWRU School of Medicine, Cleveland, OH, 44106, United States
[c] Department of Pediatrics, Rainbow Babies & Children's Hospital, CWRU School of Medicine, Cleveland, OH, 44106, United States
[d] Department of Pediatrics and Lawrence D. Long, MD Center for Perinatal Biology Loma Linda University Loma Linda, CA, United States
[e] Division of Pulmonary, Critical Care and Sleep Medicine, Louis Stokes VA Medical Center, Cleveland, OH, 44106, United States

ARTICLE INFO

Keywords:
Acute lung injury (ALI)
Nucleus tractus solitarii (nTS)
*Tractus solitarii*evoked excitatory postsynaptic current (TS-eEPSC)
Synaptic depression
Synaptic efficacy

ABSTRACT

Acute Lung Injury (ALI) alters pulmonary reflex responses, in part due to changes in modulation within the lung and airway neuronal control networks. We hypothesized that synaptic efficacy of *nucleus tractus solitarii* (nTS) neurons, receiving input from lung, airway, and other viscerosensory afferent fibers, would decrease following ALI. Sprague Dawley neonatal rats (postnatal days 9–11) were given intratracheal installations of saline or bleomycin (a well-characterized model that reproduces the pattern of ALI) and then, one week later, *in vitro* slices were prepared for whole-cell and perforated whole-cell patch-clamp experiments (postnatal days 16–21). In preparations from ALI rats, 2nd-order nTS neurons had significantly decreased amplitudes of both spontaneous and miniature excitatory postsynaptic currents (sEPSCs and mEPSCs), compared to saline controls. Rise and decay times of sEPSCs were slower in whole-cell recordings from ALI animals. Similarly, the amplitude of *tractus solitarii* evoked EPSCs (TS-eEPSCs) were significantly lower in 2nd-order nTS neurons from ALI rats. Overall these results suggest the presence of postsynaptic depression at TS-nTS synapses receiving lung, airway, and other viscerosensory afferent *tractus solitarii* input after bleomycin-induced ALI.

1. Introduction

Acute lung injury (ALI) and its most severe manifestation, acute respiratory distress syndrome (ARDS), is a common cause of acute respiratory failure and is characterized by widespread injury and inflammation of the lungs (Rubenfeld et al., 2005). Left untreated, initial injury may progress with the development of hypoxemia, systemic inflammation and potentially chronic lung damage characterized by pulmonary fibrosis, further exacerbating the pathophysiology of the patient (Ware and Matthay, 2000). As lung injury evolves, disruption of normal pulmonary physiology results in perturbations of respiratory control that alter central respiratory pattern generation, and pulmonary chemoreceptor sensitivity (Gattinoni et al., 1994; Kollef and Schuster, 1995; Jacono et al., 2006; Lieu and Undem, 2011). These changes may be adaptive, but they can also contribute to the numerous ARDS-related sequelae, including prolonged bouts of mechanical ventilation (Gajic et al., 2007; Ranieri et al., 2012).

Previous studies have shown pulmonary diseases, lung fibrosis, and ALI to be associated with (1) long-term changes in the sensitivity of pulmonary sensory receptors, (2) altered excitability at the level of neurons in the nodose ganglia, and/ or (3) altered synaptic plasticity at second-order neurons in the *nucleus tractus solitarii* (nTS) as well as higher order synapses (Schelegle et al., 2001; Undem, 2005; Bonham et al., 2006; Lieu and Undem, 2011; Jaiswal et al., 2013; Litvin et al., 2018). In this study we focused on the effect ALI has on synaptic efficacy of 2nd-order nTS neurons receiving input from lung, airway, and other viscerosensory afferent fibers traveling through the *tractus solitarii* (TS). We chose to examine the TS-nTS synapse because it is modulated in a number of pulmonary reflexes, and expresses neuroplasticity in a variety of pathophysiological conditions (Kunze, 1972; Mendelowitz,

Abbreviations: ALI, acute lung injury; nTS, *nucleus tractus solitarii*; TS, *tractus solitarii*; sEPSC, spontaneous excitatory postsynaptic current; mEPSC, miniature excitatory postsynaptic current; eEPSC, evoked excitatory postsynaptic current; PPR, paired pulse ratio

* Corresponding author at: Loma Linda University, Department of Pediatrics, Lawrence D. Long, MD Center for Perinatal Biology, 24941 Stewart St. Loma Linda, CA 92350, United States.
E-mail address: cgwilson@llu.edu (C.G. Wilson).

https://doi.org/10.1016/j.resp.2019.103250
Received 13 March 2019; Received in revised form 14 June 2019; Accepted 2 July 2019
Available online 25 July 2019
1569-9048/

1999; Joad et al., 2004; Travagli et al., 2006; Kline et al., 2007; Zhang et al., 2009; Zhang and Mifflin, 2010; Pamenter et al., 2014; Mayer et al., 2015). Recent work from our group (Litvin et al., 2018) has focused on developmental changes in the expression of nTS neuron glutamatergic receptors and how ALI impacts changes in AMPA receptors on 2nd-order nTS neurons. Our focus here is on the fundamental electrophysiological response of 2nd-order nTS neurons to ALI before and after blockade of inputs to the nTS neurons. This information is key to understanding the role that ALI plays in modifying afferent input from the lung which informs breathing rhythm generation and pattern formation. We hypothesize that 2nd-order nTS neurons decrease their sensitivity to lung, airway, and other viscerosensory afferent input with ALI. It is unclear whether decreases in synaptic efficacy manifest as changes in (1) TS presynaptic vesicle release, (2) postsynaptic number, affinity, distribution, or availability of neurotransmitter receptors, and/or (3) intrinsic postsynaptic neuronal properties (Bonham et al., 2006; Coleridge et al., 1993). In this study we evaluate whether changes in synaptic efficacy after ALI are pre- or postsynaptic.

To test our hypothesis we injured neonatal rodent lungs by intratracheal installation of bleomycin, a well-standardized and reproducible model of ALI characterized by early onset inflammation (Matute-Bello et al., 2008). Postsynaptic excitatory currents from 2nd-order neurons in the caudal area of the medial nTS were recorded in whole-cell and perforated whole-cell patch-clamp configuration in acutely isolated *in vitro* brainstem slices. Our data suggests that ALI causes postsynaptic depression by decreasing the amplitude of excitatory post-synaptic currents (EPSCs) and prolonging the rise and decay times for sEPSCs. These findings provide evidence linking ALI to postsynaptic depression at TS-nTS synapses.

2. Methods

2.1. Animals

Sprague Dawley dams with litters were purchased from ENVIGO (Indianapolis, IN, USA), and delivered at least 24 h prior to being used for the experiment. Rats were delivered pathogen free, and housed under specific-pathogen free conditions with a 12 -h light/dark cycle. All procedures were conducted in accordance with the National Institutes of Health (NIH) guidelines for care and use of laboratory animals (https://www.nap.edu/catalog/5140/guide-for-the-care-and-use-of-laboratory-animals) and were approved by the Institutional Animal Care and Use Committee at Case Western Reserve University.

2.2. Bleomycin-induced lung injury

For induction of ALI, neonatal rats were given intratracheal installations of bleomycin (Bleo) (0.5 units in 40 µl phosphate-buffered saline (PBS)) at age postnatal days 9 to 11 (P9–11) and then used for whole-cell and perforated whole-cell patch-clamp experiments between the ages of postnatal days 16 to 21 (P16–21), which is 7 to 10 days following instillation of bleomycin. As a negative control a separate group of age-matched rats received intratracheal instillation of saline (40 µl PBS). Bleomycin is an antineoplastic antibiotic drug isolated from the actinomycete *Streptomyces verticillus* and causes oxidative stress and DNA breaks, which ultimately lead to cell death (Matute-Bello et al., 2008). As previously reported, rats were sedated using an intraperitoneal injection of ketamine, xylazine, and acepromazine cocktail at 0.1 ml per 50 g body weight (Jacono et al., 2011). Rats were next placed on a sterilized surgical board, disinfected with betadine at the surgical site, and a 4 mm long midline cervical incision was made to expose the trachea. Bleomycin or saline was then instilled using a 26-gauge needle. The incision site was sealed using surgical adhesive and rats were observed during recovery and then returned to the animal facility and monitored daily until the day of the experiment.

2.3. Brainstem slice preparation

Seven to ten days after intratracheal instillation of bleomycin or saline, neonatal rats were deeply anesthetized with isoflurane and decapitated. The brainstem was removed and dissected in ice-cold artificial cerebrospinal fluid (aCSF; in mM: 124 NaCl, 3 KCl, 1.5 $CaCl_2$, 1 $MgSO_4$, 0.5 $NaHPO_4$, 25 $NaHCO_3$, 30 D-glucose, pH 7.4) infused with carbogen (95% O_2, 5% CO_2). The ventral surface of the brainstem was attached to a mounting block with cyanoacrylate (Krazy Glue®, Elmer's Products Inc., High Point, NC, USA) and firmly affixed in a vibratome (VT1000, Leica Biosystems Inc. Buffalo Grove, IL). Horizontal brainstem slices (300 µm thick) containing the TS and medial nTS in the same plane were cut in ice-cold, carbogen-gassed aCSF. Brainstem slices were quickly transferred to a polycarbonate chamber (26GLP, Warner instruments, Hamden, CT, USA) and held in place using a custom-made slice anchor consisting of a platinum ring with nylon threads. The chamber was fitted to a fixed-stage Leica DMLFS (Leica Biosystems Inc., Buffalo Grove, IL, USA) with infrared differential interference contrast (IRDIC) optics and a camera (*QImaging*, Canada) to visualize the slice. The slice was continuously perfused with carbogen-gassed aCSF held at 27 °C by an inline heater (TC-324C and SH-27B, *Warner instruments*, Hamden, CT, USA) at a rate of 3 mL per minute. The slice was kept at 27 °C to maintain its viability and allowed to equilibrate in the chamber for approximately 40 min before recordings.

2.4. NTS electrophysiological recordings of sEPSCs and mEPSCS

All electrophysiological recordings were obtained from nTS neurons that were blind patched and located in the caudal area of the medial nTS. This area of the nTs receives input from viscerosensory information, including that arising from the heart, lungs, airways, and gastrointestinal tract (Fig. 1**A**). Glass micropipettes (Borosilicate glass BF150, Sutter Instruments, Novato, CA, USA) were pulled (2–3 µm tip diameter and 6–8 MΩ resistance) using a Flaming/Brown horizontal pipette puller (P-97, *Sutter Instruments*, Novato, CA, USA) and filled with intracellular solution containing (in mM: 10 NaCl, 130 K^+-gluconate, 11 EGTA, 1 $CaCl_2$, 10 HEPES, 1 $MgCl_2$, 0.2 NaGTP, 2 MgATP, pH 7.3). Gabazine, a selective $GABA_A$ receptor antagonist, was added to the aCSF bath to block inhibitory postsynaptic currents (30 µM, SR-95531, *Sigma Aldrich*, St. Louis, MO, USA). The micropipette was attached via headstage to a patch-clamp amplifier (EPC10, *HEKA Elektronik*, Bellmore, NY, USA). The micropipette was guided to the desired area of the nTS using a motorized 3-axis micromanipulator (MP-285, *Sutter Instruments*, Novato, CA, USA).

The TS was stimulated with a concentric bipolar electrode (*FHC*, Bowdoin, ME, USA), delivering a square pulse from a stimulus isolation unit (PSIU6) attached to a stimulator (S48, *Grass Technologies/Natus Neuro*, Warwick, RI, USA). The tip of the bipolar electrode was placed directly atop the TS fiber bundle. The intensity of the TS stimulus for each recording was adapted from Kline and colleagues (Kline et al., 2009). The magnitude of the TS stimulus was increased until an evoked EPSC was observed, and the final stimulus intensity was set at 1.5 times this threshold (0.01–0.6 mA, 0.1 ms duration). NTS neurons with TS-eEPSCs exhibiting short, fixed latencies (jitter < 250 µs) were considered monosynaptically connected to the TS afferent terminals, and thus identified as 2nd-order nTS neurons (Doyle and Andresen, 2001; McDougall et al., 2009). NTS neurons with jitter ≥250 µs were excluded from analysis. Spontaneous EPSCs were recorded from 2nd-order nTS neurons for a 5-minute period, after which, tetrodotoxin (TTX) (1 µM, ab120055, *Abcam Biochemicals*, Cambridge, MA, USA) was introduced into the bath solution to, isolate spontaneous, non-action-potential-initiated vesicle release, and thus examine mEPSCs. Miniature EPSCs were defined as events that occurred when the cell failed to respond to TS-stimulation and were recorded for a 5-minute period.

These experiments were completed in the whole-cell voltage-clamp mode. NTS neurons were maintained in voltage-clamp at a holding

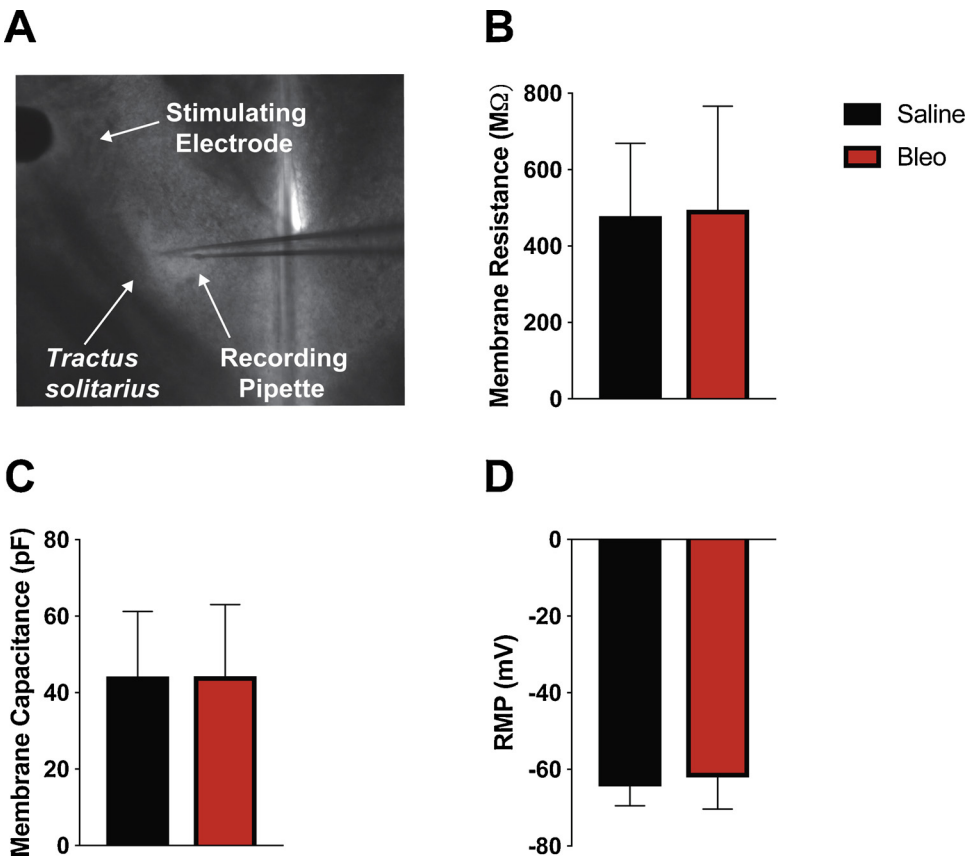

Fig. 1. A. Stimulating electrode placement and localized region of nTS patched. B–D. **Mean passive membrane properties of 2nd-order nTS neurons 7 to 10 days after intratracheal installation of bleomycin.** Data presented in this figure was collected from whole cell patched 2nd-order nTS neurons. **A.** Representative photo of the 300 µM horizontal slice with the nylon harp placed on the outer edge. The stimulating electrode was gently positioned upon the darkly striated tractus solitarii distal to the site of recording. The caudal area of the medial nTS can be seen at the tip of the recording pipette, and was visualized with DIC at 5x, and a whole cell patch was made. **B–D.** Membrane resistance (**B**), membrane capacitance (**C**) and resting membrane potential (RMP) (**D**) were recorded in Bleo (n = 11 neurons, 11 slices, 11 rats) and saline (n = 14 neurons, 14 slices, 14 rats) treated rats to determine whether acute lung injury altered the passive membrane properties of 2nd-order nTS neurons. Mean data shows that 7–10 days following bleomycin-induced lung injury there was no significant difference in the membrane resistance ($P = 0.86$), membrane capacitance ($P = 0.99$) or resting membrane potential ($P = 0.39$) between saline and Bleo groups. Data is represented as mean ± standard deviation.

potential of –65 mV during recordings. Recordings were acquired at 10 kHz, amplified using an EPC10 amplifier with "Patchmaster" software (*HEKA Elektronik*, Bellmore, NY, USA), digitized, and recorded with a *PowerLab* data acquisition system (*PowerLab* hardware and *LabChart* version 8 software, AD Instruments, Colorado Springs, CO, USA).

2.4.1. NTS electrophysiological recordings of TS-eEPSCs

In order to evaluate TS-eEPSCs at varying frequencies we used perforated whole-cell patch-clamp. This method was employed to improve long-term recording stability, reduce dilution of intracellular contents, and prevent current "run–down" (Rae et al., 1991; Lippiat, 2008; Linley, 2013). Amphotericin B solution was prepared as described by Smith and Neher (Smith and Neher, 1997; Smith, 1999). Patch pipettes were filled with the same intracellular solution as described in Section 2.4, with Amphotericin B (10 µL, A2411, *Sigma Aldrich*, St. Louis, MO, USA) added to 1 mL of intracellular solution. No Gabazine was present in the aCSF bath. The magnitude of the TS stimulus for each recording was determined, and 2nd-order nTS neurons were identified as in Section 2.4. TS-eEPSC amplitude was recorded in response to 0.5 Hz and 10 Hz stimulus trains (0.1 ms duration) to determine whether intratracheal instillation of bleomycin alters vesicle release probability from the stimulated TS presynaptic afferent fiber. This stimulation range was chosen in order to emulate the dynamic frequency range of rat peripheral chemoreceptor afferent fibers innervating the carotid body (1–10 Hz) (Vidruk et al., 2001; Kline et al., 2002), and the range of firing frequencies seen during experiments quantifying rat lung mechanoreceptor afferent fiber discharge (such as slowly adapting stretch receptor (SAR) afferent fibers, 1–16 Hz) (Schelegle et al., 2001). Stimulation ranges for carotid body chemoafferent fibers was included because carotid body sensitivity can increase after ALI even in the absence of systemic hypoxemia (Jacono et al., 2006). The paired–pulse ratio (TS-eEPSC2 amplitude/TS-eEPSC1 amplitude) of the first two TS-eEPSCs from the 0.5 Hz and 10 Hz stimulus trains was quantified. In addition, the failure rate of TS-evoked EPSCs in both the 0.5 Hz and 10 Hz stimulus trains was analyzed by comparing the percentage of TS-eEPSCs that did not reach amplitude thresholds greater than 4 standard deviations above root mean square (RMS) noise (10 pA). We also calculated the variability of the mean TS-eEPSC amplitude for 10 consecutive events of each neuron in both the 0.5 Hz and 10 Hz stimulus trains using the inverse of the coefficient of variation squared ($1/CV^2$) for Bleo and saline treated groups.

Additionally, using perforated whole-cell patch-clamp, we quantified the input resistance (R_{IN}) and frequency-current (F–I) curves of the postsynaptic neuron. R_{IN} was determined by the slope of the relation between injected hyperpolarizing currents and the resulting steady-state change in membrane potential. Current-clamp configuration was used to construct F–I curves at fixed 4.5 s intervals to measure the minimal (rheobase) and maximal current to elicit action potentials and depolarization block respectively, and assess the neuron's dynamic range. From the −65 mV holding potential (holding current varied slightly by cell) we applied a constant current of -90 pA for 500 ms followed by a ramp current for 4000 ms which resulted in depolarization blockade of action potential firing in all neurons tested. The value of the ramping current would vary by cell. The results of three consecutive current ramps were averaged to compare rheobase and maximal current before depolarization block between Bleo and saline treated groups. The instantaneous frequency of the first five and final five action potential spikes during the current ramp was also measured as an additional metric of neuronal excitability.

2.5. Data extraction for analysis and statistics

Current-ramp evoked action potentials, as well as spontaneous, miniature, and TS-evoked EPSCs that were representative of mean Bleo and saline values, were exported from *LabChart* (ADInstruments,

Colorado Springs, CO, USA) and plotted in Prism6 (*GraphPad Software* Inc., La Jolla, CA, USA) before final figure composition in Adobe Illustrator CC (Adobe Systems Inc., San Jose, CA, USA). Digital post-processing using low-pass filtering (< 2000 Hz) in *LabChart* was used to generate representative traces of short timescale (single) Bleo and saline sEPSCs and mEPSCs. These files were exported and overlayed in *AxographX* (*Axograph Software*, Berkeley, CA, USA) and then exported to *Adobe Illustrator CC*. All data processing and statistics were completed using *GraphPad Prism6* and exported to *Adobe Illustrator CC*. All data was reported as mean ± standard deviation. The probability of statistical significance was P values < 0.05.

2.5.1. Analysis of spontaneous and miniature EPSCs

Both the sEPSCs and mEPSCs were analyzed in 30-second epochs using *miniAnalysis* software (*Synaptisoft Inc.*, Decatur, GA, USA). Frequency, rise time (measured from baseline to peak), decay time (measured from baseline to peak), and amplitude of sEPSCs and mEPSCs were averaged for each patched neuron, and compared between Bleo and saline treated groups using unpaired parametric two-tailed *t*-tests. Cumulative probability plots for these parameters were generated using mini analysis software, but were not statistically compared.

2.5.2. Analysis of TS-evoked EPSCs

Two-way repeated-measured ANOVA with Sidak multiple comparison correction was used to compare 10 consecutive stimulation event numbers within the saline and Bleo groups at 0.5 Hz and 10 Hz. The paired–pulse ratio, failure rate, and $1/CV^2$ were analyzed at both 0.5 Hz and 10 Hz stimulus frequencies and compared between treatment groups (Bleo versus saline) using two-way ANOVA with Sidak multiple comparison correction.

2.5.3. Analysis of current ramps

The frequency-current relationship for each 2nd-order nTS neuron was measured using a custom macro in *Igor Pro 6* (*WaveMetrics*, Lake Oswego, OR, USA). The rheobase current and maximal current required for action potential (AP) failure (depolarization block) were averaged from three ramp trials for each cell and compared between Bleo and saline groups using an unpaired two-tailed *t*-test. The spiking frequency associated with the rheobase and maximal currents were determined by averaging the instantaneous spiking frequency of the first five and last five AP spikes across three ramp trials, and then compared using unpaired two-tailed *t*-tests. These values provided a quantifiable index of short-time scale excitability changes among 2nd-order nTS neurons between Bleo and saline groups.

3. Results

Acute lung injury did not affect the passive membrane properties of 2nd order nTS neurons as determined by comparing recordings from Bleo (n = 11 neurons, 11 slices, 11 rats) and saline (n = 14 neurons, 14 slices, 14 rats) treated groups (Fig. 1). In particular, membrane resistance (R_m) (Fig. 1**B**), membrane capacitance (C_m) (Fig. 1**C**), resting membrane potential (RMP) (Fig. 1**D**) and access resistance (R_{ACC}) were not significantly different ($P > 0.1$) between Bleo (R_m, 495 ± 272 MΩ; C_m, 44 ± 19 pF; RMP, -62 ± 8 mV; and R_{ACC}, 82 ± 27 MΩ) and saline (R_m, 478 ± 191 MΩ; C_m, 44 ± 17 pF, RMP, −64 ± 5 mV; and R_{ACC}, 95 ± 32 MΩ) treated rats. These data suggest that ALI did not affect the intrinsic membrane properties of the 2nd-order nTS neurons.

3.1. Impact of acute lung injury on spontaneous EPSCs

Representative recordings from saline and Bleo rats are displayed in Fig. 2**A**. Qualitative evaluation of superimposed single sEPSCs from both treatment groups (Fig. 2**F**) reveals differences in amplitude, as well as in rise and decay times. Our group data show a significant decrease in average amplitude of sEPSC in Bleo (11 ± 2 pA) compared to saline (15 ± 5 pA, $P = 0.03$) rats (inset of Fig. 2**B**), which is also reflected by a leftward shift in the cumulative probability plot (Fig. 2**B**). This attenuation in amplitude was accompanied by a significantly slower rise time of sEPSCs in Bleo (4.5 ± 0.8 ms) compared to saline rats (3.6 ± 0.8 ms, $P = 0.01$) (inset of Fig. 2**C**) and a significantly slower decay time of sEPSCs (inset of Fig. 2**D**) in Bleo (5.3 ± 1.6 ms) compared to saline (4.0 ± 1.3 ms $P = 0.04$) rats. These observations were reflected by a rightward shift in the cumulative probability plots of rise time and decay time respectively (Fig. 2**C** and **D**). There was also no significant difference in sEPSC frequency of neurons from Bleo (4.1 ± 2.2 Hz) compared to saline (5.0 ± 3.8 Hz, $P = 0.53$) rats (inset of Fig. 2**E**), which is also observed in the cumulative probability plot of interevent interval (IEI) (Fig. 2**E**). We used IEI as another means to represent the frequency of sEPSCs within the saline and Bleo groups. A greater frequency of sEPSCs correlates to a shorter IEI time. Data from both groups showed no correlation between rise time and amplitude or rise time and decay time in both Bleo and saline groups (**data not shown**). These sEPSC results suggest that ALI may alter the amount of excitatory neurotransmitter released from the presynaptic afferent fiber, and/or the number, clustering, and/or kinetics of the postsynaptic excitatory neurotransmitter receptors.

3.2. Impact of acute lung injury on spontaneous, non-action-potential-initiated, mEPSCs

Spontaneous EPSCs represent a mixed population of both action potential dependent and independent currents (Lee and O'Dowd, 1999). To better assess whether the decrease in sEPSC amplitude was mediated by action potential independent mechanisms, we recorded spontaneous synaptic transmission in the presence of 1 μM tetrodotoxin (TTX), a voltage–gated sodium channel blocker that inhibits action potential generation and propagation. Representative traces of mEPSCs from saline and Bleo rats are displayed in Fig. 3**A**. When qualitatively looking at a single mEPSC superimposed from both treatment groups (Fig. 3**F**) it appears that there is a difference in amplitude. Our data shows a significant decrease in the mean mEPSC amplitude in neurons from Bleo rats (10 ± 2 pA) when compared to saline rats (15 ± 6 pA, $P = 0.04$) (Fig. 3**B**). Slower rise and decay times of mEPSCs were recorded in neurons from Bleo (rise time 4.4 ± 0.9 ms; decay time 5.4 ± 1.5 ms) compared to saline (rise time 3.7 ± 1.1 ms; decay time 4.3 ± 1.5 ms) rats that was analogous to the slower rise and decay times observed in the sEPSCs. However, this difference did not achieve statistical significance (rise time: $P = 0.10$, decay time: $P = 0.10$) (Fig. 3**C** and **D**). There was no significant difference in the mean mEPSC frequency in Bleo (3.7 ± 3.0 Hz) compared to saline (3.6 ± 2.2 Hz, $P = 0.97$) rats, which is also shown by no shift in the cumulative probability plot of IEI (Fig. 3**E**). All in all, our findings strongly suggest that the sensitivity of the postsynaptic membrane to excitatory neurotransmitters (that is the number and conductance of excitatory receptors) is reduced in 2nd-order nTS neurons receiving input from TS-afferents after ALI.

3.3. Effect of ALI on EPSCs evoked by TS stimulation

To further analyze the impact of acute lung injury on synaptic transmission, we examined the properties of EPSCs evoked by TS stimulation at 0.5 and 10 Hz stimulus trains. Stimulus bursts at 0.5 Hz, revealed a significant decrease in the group mean amplitude of TS-eEPSC events in Bleo (66.3 ± 32.2 pA, n = 22 neurons, 15 slices, 15 rats) compared to saline (111.6 ± 39.9 pA, n = 10 neurons, 8 slices, 8 rats, $P < 0.01$) treated groups. (Fig. 4**A**). In contrast, at 10 Hz stimulus bursts, there was no significant difference in the group mean amplitude of TS-eEPSC events in Bleo (37 ± 20 pA, n = 22 neurons, 15 slices, 15 rats) compared to saline (48 ± 14 pA, n = 10 neurons, 8 slices, 8 rats, $P = 0.15$) treated groups (**data not shown**). When 10 consecutive

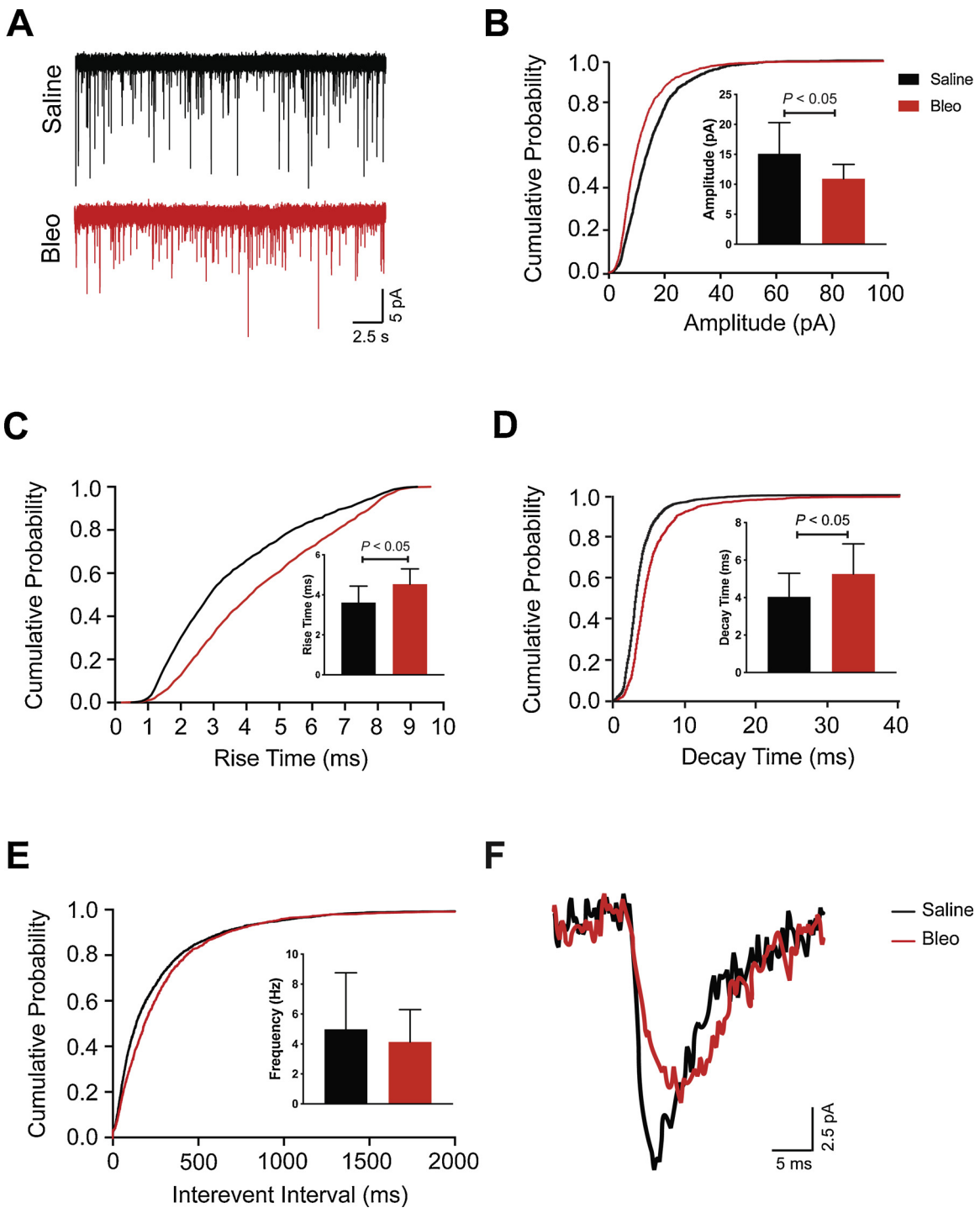

Fig. 2. Amplitude is significantly decreased, and rise and decay times are significantly slower in spontaneous EPSCs following acute lung injury. Data presented in this figure was collected from whole cell patched 2nd-order nTS neurons. **A.** Representative trace from saline and Bleo treated 2nd-order nTS neurons showing sEPSCs over the course of a 30 s epoch. **B–E.** Cumulative probability plots with inset bar graphs representing mean data ± standard deviation for sEPSC amplitude (**B**), rise time (**C**), decay time (**D**), and interevent interval (frequency) (*E*) in 2nd-order nTS neurons from Bleo and saline groups. There was a significant decrease ($P = 0.03$) in sEPSC amplitude (**B**) between Bleo and saline neurons that was reflected in a leftward shift in the cumulative probability plot. There was also a significant increase ($P = 0.01$) in sEPSC rise time (**C**) that was reflected in a rightward shift in the cumulative probability plot, and a significant increase ($P = 0.04$) in sEPSC decay time (**D**) that was reflected in a rightward shift of the cumulative probability plot. The frequency (*E*) of spontaneous sEPSCs was not significantly different ($P = 0.53$) between Bleo and saline groups. Bleo group (n = 10 neurons, 10 slices, 10 rats); saline group (n = 14 neurons, 14 slices, 14 rats). Cumulative probability plots represent analyzed cells patched from Bleo and saline treated rats. **F.** Representative trace overlaying a single sEPSC from a saline and Bleo 2nd-order nTS neuron.

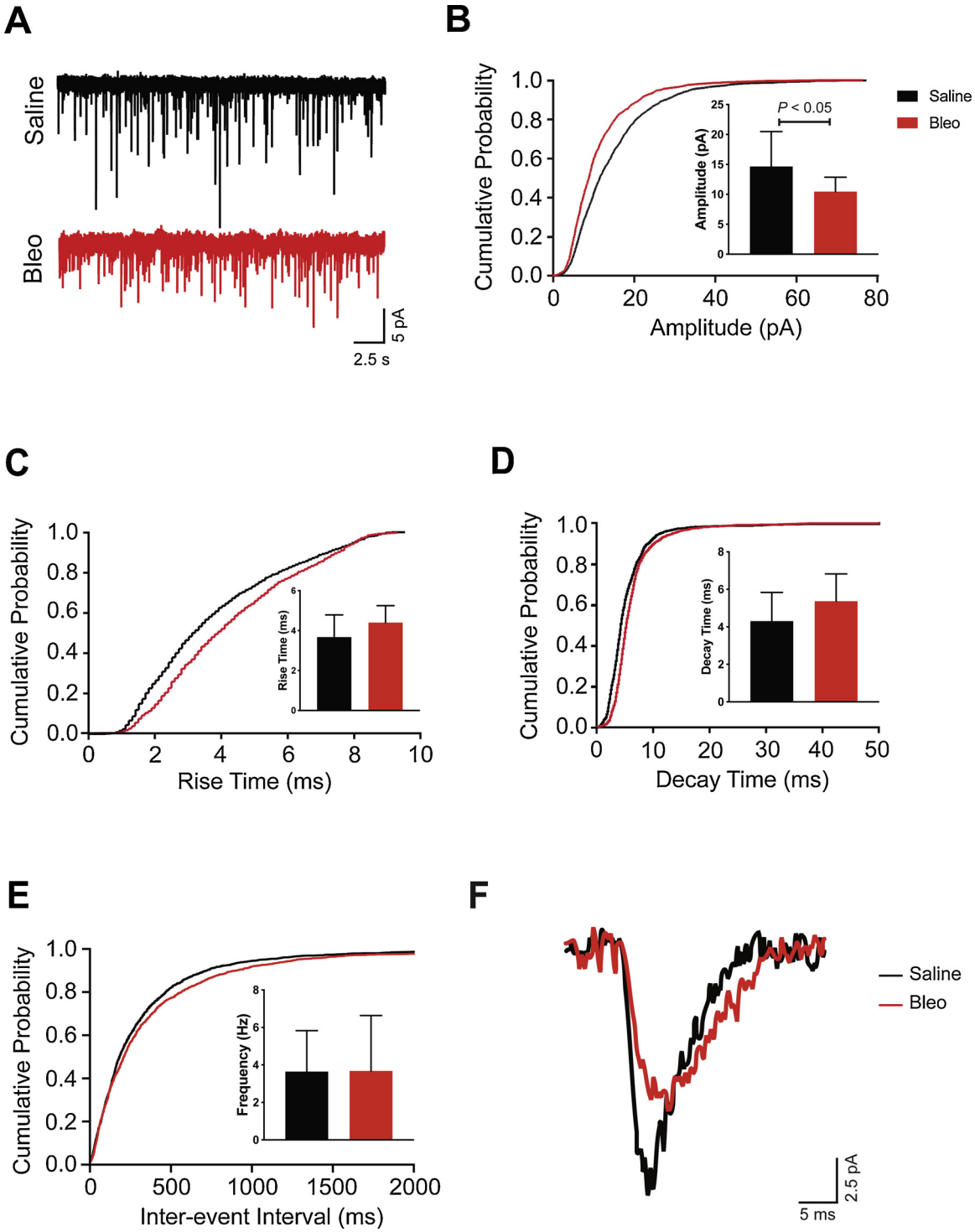

Fig. 3. Amplitude is significantly decreased in miniature EPSCs following acute lung injury. Data presented in this figure was collected from whole cell patched 2nd-order nTS neurons. **A.** Representative trace from saline and Bleo treated 2nd-order nTS neurons showing mEPSCs over the course of a 30 s epoch. **B–E.** Cumulative probability plots with inset bar graphs representing mean data ± standard deviation. (**B**) The amplitude of mEPSCs was significantly decreased ($P = 0.04$) in Bleo compared to saline treated rats (see inset), which was reflected in a leftward shift in the cumulative probability plot. A trend towards slower rise time ($P = 0.10$) (**C**) and decay time ($P = 0.10$) (**D**) of mEPSCs in Bleo compared to saline groups, but differences did not reach statistical significance. (*E*) There was no significant difference in the frequency of mEPSCs between Bleo and saline 2nd-order neurons ($P = 0.97$). Bleo group (n = 10 neurons, 10 slices, 10 rats); saline group (n = 14 neurons, 14 slices, 14 rats). Cumulative probability plots represent analyzed cells patched from Bleo and saline treated rats. **F.** Representative trace overlaying a single mEPSC from a saline and Bleo 2nd-order nTS neuron.

event amplitudes (stimulated at 0.5 Hz) were compared between Bleo and saline groups, the amplitudes were significantly decreased in 5 of 10 consecutive stimulation events ($P < 0.05$: train events 1, 3, 4, 7, and 8) (Fig. 4**B**). Additionally, there is a significant decrease in mean event amplitude *within* 10 consecutive mean evoked events stimulated at 0.5 Hz in the Bleo treated group ($P < 0.05$: mean event amplitudes for events 4, 5, 6, 7, and 8 when compared to event 1), and a significant decrease *within* 10 consecutive mean event amplitudes stimulated at

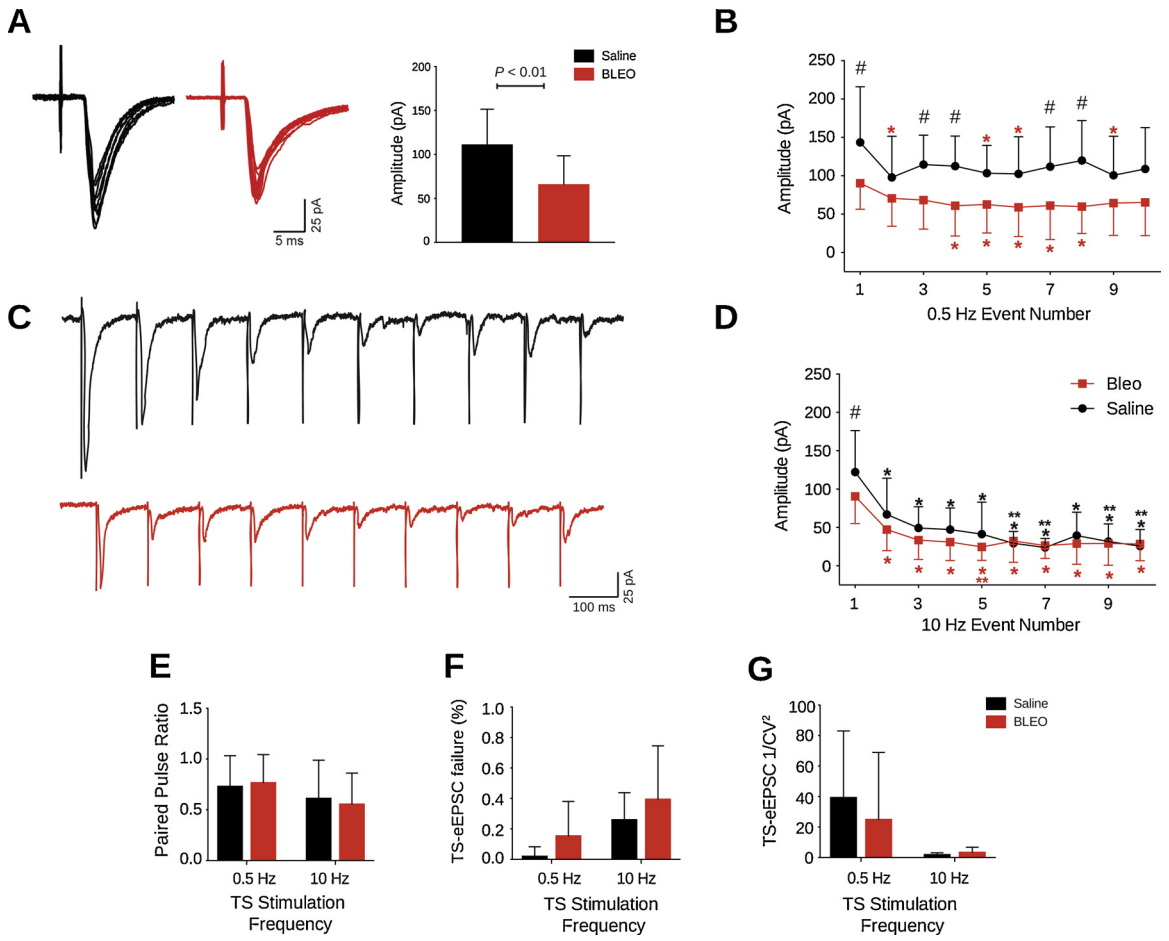

Fig. 4. Amplitude of TS-eEPSCs is significantly attenuated in rats 7 to 10 days after intratracheal installation of bleomycin at 0.5 Hz TS stimulation. Data presented in this figure was collected from perforated whole cell patched 2nd-order nTS neurons. **A.** Representative traces overlaying 0.5 Hz stimulation events from Bleo (Red) and saline (Black) treated groups. Group mean amplitude of TS-eEPSCs events in Bleo treated rats (n = 22 neurons, 15 slices, 15 rats) was significantly attenuated at 0.5 Hz TS stimulation compared to saline (n = 10 neurons, 8 slices, 8 rats, $P < 0.01$). **B.** The mean amplitude of 10 consecutive events stimulated at 0.5 Hz were significantly decreased in 5 out of 10 events in Bleo compared to saline (Symbol #: $P < 0.05$ between Bleo and saline events 1, 3, 4, 7, and 8, n = 22 for Bleo, n = 10 for saline). Within the saline treated group, the mean amplitudes of the 2nd, 5th, 6th, and 9th events were significantly decreased compared to event 1 (Symbol *: $P < 0.05$). Within the Bleo treated group, the mean amplitudes of the 4th, 5th, 6th, 7th, and 8th events were significantly decreased compared to event 1 (Symbol *: $P < 0.05$). **C.** Representative traces depicting ten consecutive individual events from saline (Black) and Bleo (Red) at 10 Hz TS-stimulation. **D.** The mean amplitude of 10 consecutive events stimulated at 10 Hz was significantly decreased at event 1 in Bleo compared to saline (Symbol #: $P < 0.01$ between Bleo and saline event 1, n = 22 for Bleo, n = 10 for saline). Within the saline treated group, the mean amplitudes of the 2nd, 3rd, 4th, 5th, 6th, 7th, 8th, 9th and 10th events was significantly decreased compared to event 1 (Symbol *: $P < 0.05$). Also within the saline group, the mean amplitudes of the 6th, 7th, 9th, and 10th events were significantly decreased compared to event 2 (Symbol **: $P < 0.05$). Within the Bleo treated group, the mean amplitudes of the 2nd, 3rd, 4th, 5th, 6th, 7th, 8th, 9th, and 10th events were significantly decreased compared to event 1 (Symbol *: P < 0.05). Also within the Bleo group, the mean amplitude of the 5th event was significantly decreased compared to event 2 (Symbol **: $P < 0.05$) **E.** Saline and Bleo treated rats showed no significant difference in paired pulse depression (EPSC2/EPSC1) at the 0.5 Hz (saline n = 10 neurons and Bleo n = 22 neurons $P = 0.74$) and 10 Hz (saline n = 10 neurons and Bleo n = 22 neurons $P = 0.65$) stimulation frequencies. **F.** Saline and Bleo treated rats showed no significant difference in TS-eEPSC failure rates at 0.5 Hz (saline n = 10 neurons and Bleo n = 22 neurons $P = 0.08$) and 10 Hz (saline n = 10 neurons and Bleo n = 22 neurons $P = 0.26$) stimulation frequencies. **G.** Saline and Bleo treated rats showed no significant difference in $1/CV^2$, a measure of EPSC variability, at 0.5 Hz (saline n = 10 neurons and Bleo n = 22 neurons $P = 0.40$) and 10 Hz (saline n = 10 neurons and Bleo n = 22 neurons $P = 0.16$) TS stimulation.

0.5 Hz in saline treated group ($P < 0.05$: mean event amplitudes at 2, 5, 6, and 9 when compared to event 1) (Fig. 4**B**). When 10 consecutive mean event amplitudes (stimulated at 10 Hz) were compared between Bleo and saline groups, the amplitudes were significantly decreased in the 1st event of a train of 10 consecutive stimulated events ($P < 0.05$: train event 1) (Fig. 4**D**). Additionally there is a significant decrease *within* 10 consecutive mean event amplitudes stimulated at 10 Hz in the Bleo treated group ($P < 0.05$: mean event amplitudes at 2, 3, 4, 5, 6, 7, 8, 9, and 10 when compared to event 1; mean event amplitude of 5 when compared to event 2), and a significant decrease *within* 10 consecutive mean event amplitudes (stimulated at 10 Hz) in the saline treated group ($P < 0.05$: mean event amplitudes at 2, 3, 4, 5, 6, 7, 8, 9, and 10 when compared to event 1; mean event amplitudes 6, 7, 9, and 10 when compared to event 2) (Fig. 4**D**). Analysis of the paired–pulse ratio (PPR) between events 1 and 2 indicated similar magnitudes of paired–pulse depression (PPR < 1) in both groups and across stimulation frequencies–Bleo *vs.* saline at 0.5 Hz (0.77 ± 0.28 (n = 22 neurons) *vs.* 0.73 ± 0.30 (n = 10 neurons), $P = 0.74$), and Bleo *vs.* saline at 10 Hz (0.56 ± 0.31 (n = 22 neurons) *vs.* 0.61 ± 0.38 (n = 10 neurons), $P = 0.65$) (Fig. 4**E**). Furthermore, the TS-eEPSC failure rate (R_F) was calculated as the probability that the TS-eEPSC amplitude is greater than or equal to 25 pA and showed no significant difference when comparing Bleo *vs.* saline at 0.5 Hz (0.15 ± 0.23 (n = 22 neurons) *vs.* 0.02 ± 0.06 (n = 10 neurons), $P = 0.08$) and 10 Hz (0.40 ± 0.35 (n = 22 neurons) *vs.* 0.26 ± 0.18 (n = 10 neurons), $P = 0.26$) (Fig. 4**F**). Finally, the inverse square of the coefficient of

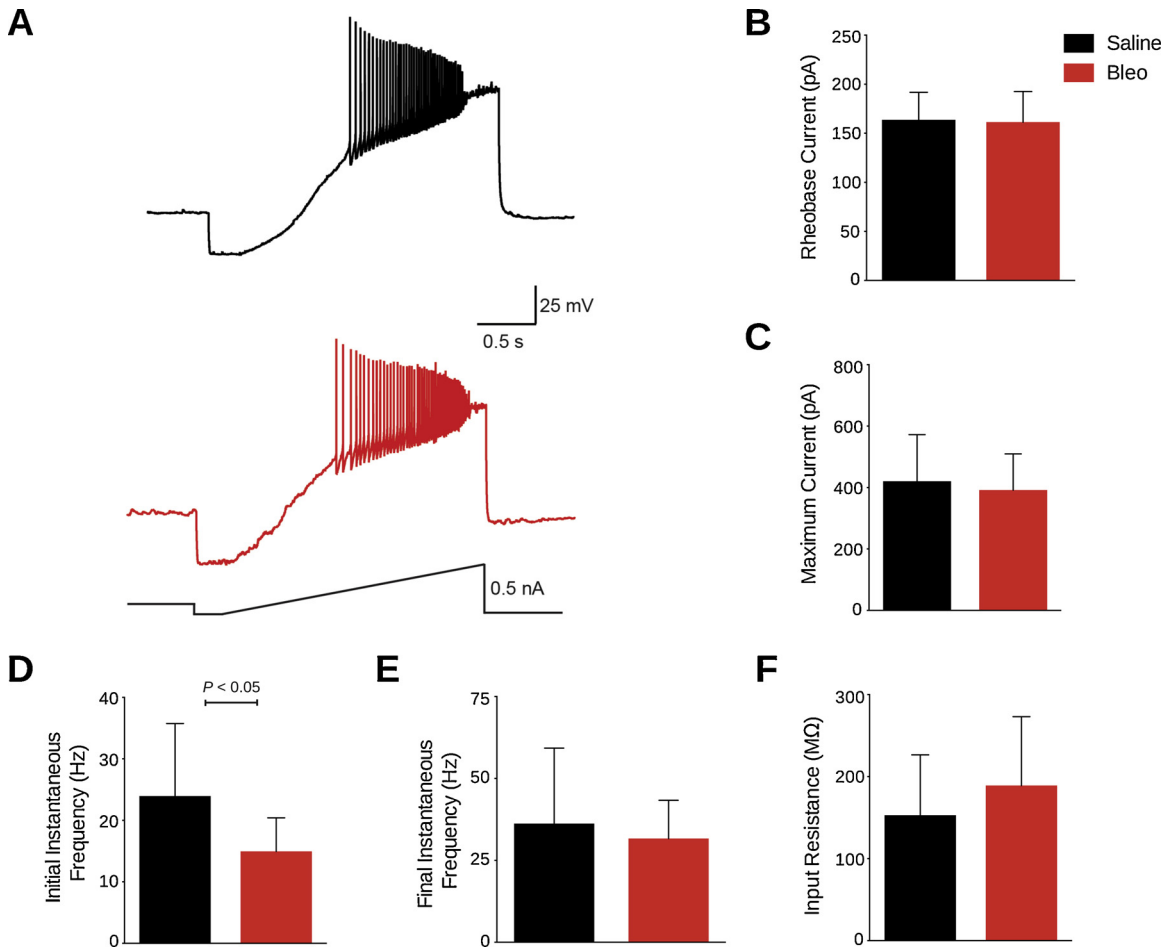

Fig. 5. Acute lung injury does not alter the intrinsic excitability of perforated whole cell patched 2nd-order nTS neurons. A. Representative F–I traces from perforated whole cell patched 2nd-order nTS neurons in saline (Black) and Bleo (Red) showing action potentials in response to increasing current until depolarization block is reached. **B–E.** (**B**) There was no significant difference in the rheobase current ($P = 0.85$), which is the minimal current required to generate an action potential, between Bleo and saline treated groups. (**C**) There was also no significant difference in the maximum current required to produce a depolarization block, thereby terminating action potential generation ($P = 0.57$). (**D**) There was a significant different in the action potential firing frequency at the rheobase current ($P < 0.05$) between Bleo and saline treated rats. (*E*) However there was no significant different in the maximum current ($P = 0.47$) between Bleo and saline treated rats. (**F**) There was no significant difference in the input resistance between Bleo and saline treated rats ($P = 0.23$). Bleo treated group had n = 21 neurons, 15 slices, 15 rats, and in the saline group n = 10 neurons, 8 slices, 8 rats. Data presented as mean ± standard deviation.

variation ($1/CV^2$) or EPSC variability of the mean TS-eEPSC amplitude, was not significantly reduced at 0.5 Hz in Bleo *vs*. saline (25.1 ± 43.9 (n = 22 neurons) *vs*. 39.4 ± 43.6 (n = 10 neurons), $P = 0.40$) treated rats, or at 10 Hz in Bleo *vs*. saline (3.49 ± 3.28 (n = 22 neurons) *vs*. 1.94 ± 1.21 (n = 10 neurons), $P = 0.16$) treated rats (Fig. 4**G**). This suggests that intratracheal instillation of bleomycin to induce acute lung injury, does not effect the number of vesicles released from the presynaptic terminal during high frequency stimulation. We formed this conclusion because PPR, TS-eEPSC R_F, and $1/CV^2$ analyses strongly suggests that it is not a presynaptic effect even though the two-way repeated-measured ANOVA suggests the presence of a presynaptic effect, and use-dependent depression.

3.4. Effect of ALI on intrinsic excitability of postsynaptic 2nd-order nTS neurons

Finally, we sought to determine whether bleomycin-induced postsynaptic depression might be associated with changes in intrinsic excitability of the postsynaptic 2nd-order nTS neuron. We found no significant difference in the input resistance between Bleo (189 ± 84 MΩ, n = 21 neurons, 15 slices, 15 rats) versus saline (153 ± 74 MΩ; n = 10 neurons, 8 slices, 8 rats; $P = 0.23$) (Fig. 5**F**). There was also no significant difference in the rheobase current (Fig. 5**B**) between Bleo (161 ± 31 pA) versus saline (164 ± 28 pA; $P = 0.85$) or in the maximum current before depolarization block (Fig. 5**C**) between Bleo (392 ± 118 pA) versus saline (420 ± 152 pA; $P = 0.57$). There was, however, a significant difference in the initial action potential (AP) spiking frequency at the rheobase current (Fig. 5**D**) for Bleo (14.9 ± 5.5 Hz) versus saline (24.0 ± 11.8 Hz; $P < 0.05$). There was not a significant difference in the final AP spiking frequency at the maximal current (Fig. 5**E**) for Bleo (31.7 ± 11.7 Hz) versus saline (36.2 ± 23.1 Hz; $P = 0.47$) groups. This data suggests that the overall depression of excitatory neurotransmission appears to occur in the absence of major changes in intrinsic excitability following bleomycin-induced acute lung injury.

4. Discussion

4.1. Summary of findings

In this study, we examined changes in synaptic efficacy and excitability of 2nd-order nTS neurons receiving input from lung, airway, and other viscerosensory afferent fibers traveling through the *solitary tract* seven to ten days after intratracheal instillation of bleomycin. Our data shows that acute lung injury depresses postsynaptic transmission at 2nd-order nTS neurons that is associated with slower rise and decay

times of sEPSCs, and a reduction in the amplitude of excitatory post-synaptic currents measured during: (1) spontaneous release (2) TS-evoked release and (3) spontaneous, non-action-potential initiated release. Slower rise and decay times of sEPSCs after ALI may be suggestive of (1) changes in association rate constants for excitatory post-synaptic receptors, such as the α-amino-3-hydroxy-5-methyl-4-isoxazolepropionic-acid receptors (AMPARs) and N-methyl-D-aspartate receptors (NMDARs) though we did not assess any changes in these receptors in this study; and/or (2) slower excitatory transmitter exchange rate, which might be due to changes in morphological properties, glial ensheathment, or transmitter reuptake rate. In addition, slower rise time after ALI may be due to changes in NMDAR and/or AMPAR clustering, resulting in desynchronized activation of NMDARs and/or AMPARs (Frech et al., 2001). Previous studies also demonstrated that postsynaptic loss of AMPAR density and/or changes in subunit composition can produce sEPSC/mEPSC amplitude reductions (Nabekura et al., 2002; Joshi et al., 2004; Fu et al., 2005; Stincic and Frerking, 2015).

In addition, we observed no significant changes in the frequency of either sEPSCs or mEPSCs. These findings suggest that ALI did not significantly affect the releasable pool of vesicles from TS afferent terminals, or other local excitatory neurons. Furthermore, analysis of TS-eEPSCs showed no significant changes in the paired–pulse ratio, magnitude of frequency dependent depression, failure rate, or TS-eEPSC amplitude variability in Bleo versus saline rats. Taken together, these results strongly suggest that decreases in presynaptic release probability (P_R) and/or number of release sites at TS and non-TS synapses were not responsible for the amplitude reductions of 2nd-order postsynaptic EPSCs in lung injured rats (Malinow and Tsien, 1990; Zucker and Regehr, 2002; Branco and Staras, 2009).

Given the evidence of postsynaptic depression in 2nd-order nTS neurons after ALI, we sought to determine whether bleomycin-induced acute lung injury promoted changes in the intrinsic excitability of the 2nd-order postsynaptic neuron. If present, these changes might be interpreted as both compensatory and/or complimentary to the altered excitatory postsynaptic currents (Chen et al., 2003; Kline et al., 2007). However, no significant changes in resting membrane potential, input resistance, membrane capacitance or membrane resistance were identified following lung injury. Furthermore, there were no significant differences in rheobase current or maximal current required for depolarization blockade in Bleo versus saline rats. There was, however, a significant difference in the initial AP discharge frequency during the current ramp, but no significant difference in the final AP discharge frequency. Although synaptic strength reduction at TS-nTS synapses likely influences the postsynaptic neuron's ability to generate TS-dependent action potentials, ALI does not appear to produce major changes in the passive membrane properties of the postsynaptic neuron governing action potential generation (Kline et al., 2007).

4.2. Neural Inflammation as the potential mechanism for decreased synaptic efficacy at 2nd-order postsynaptic nTS neurons following ALI

Acute lung injury initiates an inflammatory cascade that includes release of proinflammatory mediators and recruitment of neutrophils to the lungs, which results in production of early response cytokines, such as interleukin (IL)-1β and tumor necrosis factor (TNF)-α (Jacono et al., 2011). This peripheral production of cytokines in the lungs is accompanied by a central neuronal inflammatory response that results in alterations in synaptic transmission in the nTS (Marty et al., 2008; Jacono et al., 2011). Litvin and colleagues showed that lung injury regulates the efficacy of 2nd-order nTS synapses through immune-mediated plasticity-like mechanisms (Litvin et al., 2018). Their work focused on developmental changes in the expression of glutamatergic receptors and how ALI impacts changes in AMPA receptors on 2nd-order nTS neurons. While they did not, specifically, focus on the intrinsic excitability of 2nd-order nTS neurons after ALI, our work provides insight into the fundamental electrophysiological response of 2nd-order nTS neurons to ALI before and after blockade of inputs to the nTS neurons. We restricted our work to assessing synaptology and gain changes as a result of bleo-induced ALI. Our results show that following ALI, this centrally mediated widespread production and/or recruitment of proinflammatory cytokines may be due to postsynaptic depression at 2nd-order nTS neurons. Our data strongly suggests that the neuroinflammatory response is via a postsynaptic mechanism since we see a significant depression in amplitude of sEPSCs, mEPSCS, and TS-eEPSCs without a loss in frequency of mEPSCs measured. Since we see this depression in all types of postsynaptic 2nd-order nTS neurons, we speculate that the neural inflammation of bleomycin-induced ALI is globally mediated, and not limited to 2nd-order nTS neurons receiving pulmonary afferent input. Our data also suggests that neural inflammation is not acting by modifying the expression, trafficking, or function of one or more ion channels, such as voltage-gated sodium and/or potassium channels, or their subunits, since we observed no major significant changes in intrinsic neuronal excitability of 2nd-order postsynaptic neurons was observed (Bonham et al., 2006).

4.3. Other possible mechanisms suggested to alter synaptic plasticity of nTS neurons

Our findings strongly suggest that bleomycin-induced lung injury leads to postsynaptic depression in 2nd-order nTS neurons receiving lung, airway, and other viscerosensory afferent input. However, our findings do not exclude the possibility that presynaptic or other modulatory inputs on 2nd-order nTS neurons may also play a role in modifying this neural circuit. Similar changes in synaptic efficacy have been shown to arise through reductions in: (1) vesicular filling, (2) asynchronous vesicular release, (3) active synapse number, as well as increases in (4) dendritic filtering, and (5) glutamate transport by astrocytes (Malinow and Tsien, 1990; Rose and Call, 1992; Takahashi et al., 1995; Bekkers and Clements, 1999; Sulzer and Pothos, 2000; Zhou et al., 2000; Zhang et al., 2014; Murphy-Royal et al., 2015). Moreover, it is possible that these adaptations are occurring at both TS- and non-TS terminals, although the presence of reduced TS-eEPSC amplitudes seen in our results makes it very likely that TS-terminals are the main area for these adaptations following ALI.

Other pathophysiological conditions can promote long-term synaptic changes at TS-nTS synapses similar to the present findings. For example, chronic intermittent hypoxia (CIH) has been shown to reduce TS-eEPSC amplitudes in nTS neurons (Kline et al., 2007; Almado et al., 2012; Mayer et al., 2015). In particular, Kline et al. identified a CIH-induced reduction in pre-synaptic P_R, while Almado and colleagues, showed that CIH could depress TS-afferent neurotransmission by a reduction in the number of available quanta (n) (Kline et al., 2007; Almado et al., 2012). In both studies a significant reduction in $1/CV^2$ was observed in rats exposed to CIH. However, in our experiments, lung injury did not alter $1/CV^2$. Furthermore, unlike the response to bleomycin-induced lung injury and CIH, chronic sustained hypoxia (CSH) promoted greater TS-eEPSC amplitudes that were associated with augmented glutamate evoked inward currents at TS-receiving neurons originating from the carotid body (Zhang et al., 2009).

4.4. Differences in nTS synaptic plasticity among acute and chronic lung injuries

Our findings report that acute lung injury leads to postsynaptic changes in the nTS. Previous studies have shown synaptic plasticity at TS-nTS synapses following chronic lung injury. In a model of extended secondhand tobacco smoke exposure in guinea pigs, Sekizawa et al. identified paired–pulse facilitation without changes in the initial evoked response or spontaneous transmission (Sekizawa et al., 2008a, 2008b). It was also shown that chronic ozone exposure in rhesus macaque primates promotes a diminution of neuronal action potential

firing frequency in response to TS stimulation (Chen et al., 2003). Our results suggest that the underlying mechanisms responsible for synaptic changes in the nTS during acute (bleomycin-induced) lung injury are different than those responsible for the changes due to chronic lung injury. This is not a surprising conclusion, given that acute and chronic intermittent hypoxia also acts differentially to elicit plasticity of nTS synaptic transmission (Kline et al., 2007; Zhang et al., 2009).

4.5. Alterations in respiratory control and ventilatory pattern variability as a result of lung injury

Changes in ventilatory control following lung injury could be compensatory and/or pathologic in nature. Previous work has shown altered respiratory control following lung injury including; (1) augmented bronchopulmonary c-fiber activity in the nTS after chronic exposure to tobacco smoke, and (2) enhanced volume sensitivity of slowly adapting stretch receptors and a blunting of the Herring-Breuer inflation reflex after chronic lung injury due to bleomycin (Mutoh et al., 2000; Schelegle et al., 2001). In addition, researchers showed acute lung injury leads to changes to ventilatory pattern variability (VPV) in rats (Jacono et al., 2011). Although these changes in the respiratory pattern are in large part due to altered pulmonary pathophysiology, hypoxemia, and reduced lung compliance, a central contribution to VPV has been postulated, with evidence of the nTS contributing to shaping VPV (Kelsen et al., 1982; Jacono, 2013). Work by Dhingra et al. showed that the vagus nerve contributes to nonlinear variability of the respiratory pattern, and that a loss of vagal input promotes a reduction in breathing pattern variability (Dhingra et al., 2011). Consequently, second-order synapses involved in the integration of viscerosensory information at the nTS are also likely involved in shaping ventilatory pattern variability. Our results suggest that changes in ventilatory pattern variability following acute lung injury may involve decreased synaptic efficacy at postsynaptic 2nd-order nTS neurons receiving lung, airway, and other viscerosensory afferent input.

4.6. Limitations of the present work

There are several limitations to our study. First, we focused our investigation on short, fixed latency synapses in the nTS. Thus, we are not able to ascertain if synaptic changes also occurred at high jitter synapses, which are likely not monosynaptic but pauci- or poly-synaptic (Accorsi-Mendonça et al., 2011). In addition, other studies have shown that lung injury alters the hypoxic sensitivity of the carotid body, gastric, and baroreceptor vagal afferents that terminate in adjacent subnuclei of the nTS (Travagli et al., 2003, 2006; Jacono et al., 2006). Therefore the EPSCs we measured may have arisen from primary afferent fibers of pulmonary, chemosensory, barosensory or even gastric origin, or from neighboring nTS neurons in the slice (Travagli et al., 2006; Sekizawa et al., 2008a; Zhang et al., 2009; Accorsi-Mendonça et al., 2011). To address this, we would need to tract trace by labeling pulmonary afferent fibers in order to specifically patch 2nd-order nTS neurons that received input from the lungs. This would allow us to further characterize these changes in EPSCs as originating solely from pulmonary afferent fibers. We also did not determine whether the decreased TS-eEPSC amplitude had an effect on the action potential firing of the postsynaptic neuron, as was observed following chronic ozone exposure (Chen et al., 2003). The relatively minor changes we observed in sEPSCs after TTX blockade may reflect a role for inflammation-induced COX2 activation and a resulting change in EP receptor inputs modulating the excitability of the nTS neurons **(**Marty et al., 2008**)** and we did not assess the role of EP receptors in these experiments. Because nTS neurons have small somata and an extensive dendritic arbor, an additional caveat is we are limited in our ability to space-clamp these neurons though we presume that there were not morphological changes that would alter the dendritic tree in bleo-treated animals. We did not assess the role of individual conductances that are known to contribute to changes in nTS neuron excitability (*e.g.* IA, TASK channels, *etc*.) nor the role that ligand-gated channels (AMPAR, NMDAR, GABAR) play in modifying nTS neuron activity. Finally, we did not precisely determine the mechanism(s) of synaptic depression, beyond the fact that changes occurred at the level of the postsynaptic neuron in the setting of acute lung injury. It is likely that multiple mechanisms are responsible in part for the reduced synaptic efficacy during lung injury, and that the relative contribution of each of these varies over time. Determining the role of these and other mechanisms in neuroplastic changes in the nTS during acute lung injury will be the focus of future studies.

4.7. Conclusions

These findings suggest that acute lung injury reduces the ability of postsynaptic 2nd-order nTS neurons to respond to neurotransmitters released from presynaptic afferent fibers. However, we do not know whether this decrease in the responsiveness of the postsynaptic neuron is due to changes in the expression level or kinetics of the postsynaptic excitatory receptors and/or expression of accessory transporters that were not present prior to bleomycin installation. Further work will need to be done to determine the mechanism(s) by which this postsynaptic depression occurs.

Author contributions

P.M.G., C.G.W. and F.J.J. contributed to the conception and design of research; P.M.G. and C.A.M performed experiments; P.M.G. and C.A.M analyzed data; P.M.G., C.A.M, C.G.W. P.M.M and F.J.J. interpreted results; F.J.J drafted the manuscript; P.M.G., C.A.M, C.G.W. P.M.M and F.J.J. edited and revised the manuscript; P.M.G., C.A.M, C.G.W. P.M.M and F.J.J. approved the final version of the manuscript.

Declaration of Competing Interest

No conflicts of interest, financial or otherwise, are declared by the authors.

Acknowledgements

This research was supported by grants from the National Institutes of Health (HL007913 and T32 HL007913) and by Award Number I01BX000873 from the Biomedical Laboratory Research & Development Service of the VA Office of Research and Development.

References

Accorsi-Mendonça, D., Castania, J.A., Bonagamba, L.G.H., Machado, B.H., Leão, R.M., 2011. Synaptic profile of nucleus tractus solitarius neurons involved with the peripheral chemoreflex pathways. Neuroscience 197, 107–120. https://doi.org/10.1016/j.neuroscience.2011.08.054.

Almado, C.E.L., Machado, B.H., Leão, R.M., 2012. Chronic intermittent hypoxia depresses afferent neurotransmission in NTS neurons by a reduction in the number of active synapses. J. Neurosci. 32, 16736–16746. https://doi.org/10.1523/JNEUROSCI.2654-12.2012.

Bekkers, J.M., Clements, J.D., 1999. Quantal amplitude and quantal variance of strontium-induced asynchronous EPSCs in rat dentate granule neurons. J. Physiol. (Paris) 516 (Pt 1), 227–248. https://doi.org/10.1111/j.1469-7793.1999.227aa.x.

Bonham, A.C., Chen, C.-Y., Sekizawa, S.-I., Joad, J.P., 2006. Plasticity in the nucleus tractus solitarius and its influence on lung and airway reflexes. J. Appl. Physiol. 101, 322–327. https://doi.org/10.1152/japplphysiol.00143.2006.

Branco, T., Staras, K., 2009. The probability of neurotransmitter release: variability and feedback control at single synapses. Nat. Rev. Neurosci. 10, 373–383. https://doi.org/10.1038/nrn2634.

Chen, C.-Y., Bonham, A.C., Plopper, C.G., Joad, J.P., 2003. Neuroplasticity in nucleus tractus solitarius neurons after episodic ozone exposure in infant primates. J. Appl. Physiol. 94, 819–827. https://doi.org/10.1152/japplphysiol.00552.2002.

Coleridge, J.C., Coleridge, H.M., Schelegle, E.S., Green, J.F., 1993. Acute inhalation of ozone stimulates bronchial C-fibers and rapidly adapting receptors in dogs. J. Appl. Physiol. 74, 2345–2352.

Dhingra, R.R., Jacono, F.J., Fishman, M., Loparo, K.A., Rybak, I.A., Dick, T.E., 2011. Vagal-dependent nonlinear variability in the respiratory pattern of anesthetized,

spontaneously breathing rats. J. Appl. Physiol. 111, 272–284. https://doi.org/10.1152/japplphysiol.91196.2008.
Doyle, M.W., Andresen, M.C., 2001. Reliability of monosynaptic sensory transmission in brain stem neurons in vitro. J. Neurophysiol. 85, 2213–2223.
Frech, M.J., Pérez-León, J., Wässle, H., Backus, K.H., 2001. Characterization of the spontaneous synaptic activity of amacrine cells in the Mouse Retina. J. Neurophysiol. 86, 1632–1643. https://doi.org/10.1152/jn.2001.86.4.1632.
Fu, Z., Logan, S.M., Vicini, S., 2005. Deletion of the NR2A subunit prevents developmental changes of NMDA-mEPSCs in cultured mouse cerebellar granule neurones. J. Physiol 563, 867–881. https://doi.org/10.1113/jphysiol.2004.079467.
Gajic, O., Afessa, B., Thompson, B.T., Frutos-Vivar, F., Malinchoc, M., Rubenfeld, G.D., Esteban, A., Anzueto, A., Hubmayr, R.D., 2007. Prediction of death and prolonged mechanical ventilation in acute lung injury. Crit Care 11, R53 doi:cc5909 [pii] \r10.1186/cc5909.
Gattinoni, L., Bombino, M., Pelosi, P., Lissoni, A., Pesenti, A., Fumagalli, R., Tagliabue, M., 1994. Lung structure and function in different stages of severe adult respiratory distress syndrome. JAMA 271, 1772–1779. https://doi.org/10.1001/jama.1994.03510460064035.
Jacono, F.J., 2013. Control of ventilation in COPD and lung injury. Respir. Physiol. Neurobiol. 189, 371–376. https://doi.org/10.1016/j.resp.2013.07.010.
Jacono, F.J., Mayer, C.A., Hsieh, Y.-H., Wilson, C.G., Dick, T.E., 2011. Lung and brainstem cytokine levels are associated with breathing pattern changes in a rodent model of acute lung injury. Respir. Physiol. Neurobiol. 178, 429–438. https://doi.org/10.1016/j.resp.2011.04.022.
Jacono, F.J., Peng, Y.-J., Nethery, D., Faress, J.A., Lee, Z., Kern, J.A., Prabhakar, N.R., 2006. Acute lung injury augments hypoxic ventilatory response in the absence of systemic hypoxemia. J. Appl. Physiol. 101, 1795–1802. https://doi.org/10.1152/japplphysiol.00100.2006.
Jaiswal, S.J., Pilarski, J.Q., Harrison, C.M., Fregosi, R.F., 2013. Developmental nicotine exposure alters AMPA neurotransmission in the hypoglossal motor nucleus and pre-Botzinger complex of neonatal rats. J. Neurosci. 33, 2616–2625. https://doi.org/10.1523/JNEUROSCI.3711-12.2013.
Joad, J.P., Munch, P.A., Bric, J.M., Evans, S.J., Pinkerton, K.E., Chen, C.-Y., Bonham, A.C., 2004. Passive smoke effects on cough and airways in young guinea pigs: role of brainstem substance P. Am. J. Respir. Crit. Care Med. 169, 499–504. https://doi.org/10.1164/rccm.200308-1139OC.
Joshi, I., Shokralla, S., Titis, P., Wang, L.-Y., 2004. The role of AMPA receptor gating in the development of high-fidelity neurotransmission at the calyx of held synapse. J. Neurosci. 24, 183–196. https://doi.org/10.1523/JNEUROSCI.1074-03.2004.
Kelsen, S.G., Shustack, A., Hough, W., 1982. The effect of vagal blockade on the variability of ventilation in the awake dog. Respir. Physiol. 49, 339–353. https://doi.org/10.1016/0034-5687(82)90121-9.
Kline, D.D., Takacs, K.N., Ficker, E., Kunze, D.L., 2002. Dopamine modulates synaptic transmission in the nucleus of the solitary tract. J. Neurophysiol. 88, 2736–2744. https://doi.org/10.1152/jn.00224.2002.
Kline, D.D., Ramirez-Navarro, A., Kunze, D.L., 2007. Adaptive depression in synaptic transmission in the nucleus of the solitary tract after in vivo chronic intermittent hypoxia: evidence for homeostatic plasticity. J. Neurosci. 27, 4663–4673. https://doi.org/10.1523/JNEUROSCI.4946-06.2007.
Kline, D.D., Hendricks, G., Hermann, G., Rogers, R.C., Kunze, D.L., 2009. Dopamine inhibits N-Type channels in visceral afferents to reduce synaptic transmitter release under normoxic and chronic intermittent hypoxic conditions. J. Neurophysiol. 101, 2270–2278. https://doi.org/10.1152/jn.91304.2008.
Kollef, M.H., Schuster, D.P., 1995. The acute respiratory distress syndrome. N. Engl. J. Med. 332, 27–37. https://doi.org/10.1056/NEJM199501053320106.
Kunze, D.L., 1972. Reflex discharge patterns of cardiac vagal efferent fibres. J. Physiol. 222, 1–15.
Lee, D., O'Dowd, D.K., 1999. Fast excitatory synaptic transmission mediated by nicotinic acetylcholine receptors in Drosophila neurons. J. Neurosci. 19, 5311–5321.
Lieu, T., Undem, B.J., 2011. Neuroplasticity in vagal afferent neurons involved in cough. Pulm. Pharmacol. Ther. 24, 276–279. https://doi.org/10.1016/j.pupt.2011.02.003.
Linley, J.E., 2013. Perforated whole-cell patch-clamp recording. Methods Mol. Biol. 998, 149–157. https://doi.org/10.1007/978-1-62703-351-0_11.
Lippiat, J.D., 2008. Whole-cell recording using the perforated patch clamp technique. Methods Mol. Biol. 491, 141–149. https://doi.org/10.1007/978-1-59745-526-8-11.
Litvin, D.G., Dick, T.E., Smith, C.B., Jacono, F.J., 2018. Lung-injury depresses glutamatergic synaptic transmission in the nucleus tractus solitarii via discrete age-dependent mechanisms in neonatal rats. Brain Behav. Immun. 70, 398–422. https://doi.org/10.1016/j.bbi.2018.03.031.
Malinow, R., Tsien, R.W., 1990. Presynaptic enhancement shown by whole-cell recordings of long-term potentiation in hippocampal slices. Nature 346, 177–180. https://doi.org/10.1038/346177a0.
Marty, V., Hachmane, M.E., Amédée, T., 2008. Dual modulation of synaptic transmission in the nucleus tractus solitarius by prostaglandin E2 synthesized downstream of IL-1β. Eur. J. Neurosci. 27, 3132–3150. https://doi.org/10.1111/j.1460-9568.2008.06296.x.
Matute-Bello, G., Frevert, C.W., Martin, T.R., 2008. Animal models of acute lung injury. Am. J. Physiol. Lung Cell Mol. Physiol. 295, L379–L399. https://doi.org/10.1152/ajplung.00010.2008.
Mayer, C.A., Wilson, C.G., MacFarlane, P.M., 2015. Changes in carotid body and nTS neuronal excitability following neonatal sustained and chronic intermittent hypoxia exposure. Respir. Physiol. Neurobiol. 205, 28–36. https://doi.org/10.1016/j.resp.2014.09.015.
McDougall, S.J., Peters, J.H., Andresen, M.C., 2009. Convergence of cranial visceral afferents within the solitary tract nucleus. J. Neurosci. 29, 12886–12895. https://doi.org/10.1523/JNEUROSCI.3491-09.2009.
Mendelowitz, D., 1999. Advances in parasympathetic control of heart rate and cardiac function. News Physiol. Sci. 14, 155–161.
Murphy-Royal, C., Dupuis, J.P., Varela, J.A., Panatier, A., Pinson, B., Baufreton, J., Groc, L., Oliet, S.H.R., 2015. Surface diffusion of astrocytic glutamate transporters shapes synaptic transmission. Nat. Neurosci. 18, 219–226. https://doi.org/10.1038/nn.3901.
Mutoh, T., Joad, J.P., Bonham, A.C., 2000. Chronic passive cigarette smoke exposure augments bronchopulmonary C-fibre inputs to nucleus tractus solitarii neurones and reflex output in young guinea-pigs. J. Physiol. 523 (Pt 1), 223–233. https://doi.org/10.1111/j.1469-7793.2000.00223.x.
Nabekura, J., Ueno, T., Katsurabayashi, S., Furuta, A., Akaike, N., Okada, M., 2002. Reduced NR2A expression and prolonged decay of NMDA receptor-mediated synaptic current in rat vagal motoneurons following axotomy. J. Physiol. 539, 735–741. https://doi.org/10.1113/jphysiol.2001.013379.
Pamenter, M.E., Carr, J.A., Go, A., Fu, Z., Reid, S.G., Powell, F.L., 2014. Glutamate receptors in the nucleus tractus solitarius contribute to ventilatory acclimatization to hypoxia in rat. J. Physiol. 592, 1839–1856. https://doi.org/10.1113/jphysiol.2013.268706.
Rae, J., Cooper, K., Gates, P., Watsky, M., 1991. Low access resistance perforated patch recordings using amphotericin B. J. Neurosci. Methods 37, 15–26. https://doi.org/10.1016/0165-0270(91)90017-T.
Ranieri, V.M., Rubenfeld, G.D., Thompson, B.T., Ferguson, N.D., Caldwell, E., Fan, E., Camporota, L., Slutsky, A.S., 2012. Acute respiratory distress syndrome: the Berlin Definition. JAMA 307, 2526–2533. https://doi.org/10.1001/jama.2012.5669.
Rose, G.J., Call, S.J., 1992. Evidence for the role of dendritic spines in the temporal filtering properties of neurons: the decoding problem and beyond. Proc. Natl. Acad. Sci. U.S.A. 89, 9662–9665.
Rubenfeld, G.D., Caldwell, E., Peabody, E., Weaver, J., Martin, D.P., Neff, M., Stern, E.J., Hudson, L.D., 2005. Incidence and outcomes of acute lung injury. N. Engl. J. Med. 353, 1685–1693. https://doi.org/10.1056/NEJMoa050333.
Schelegle, E.S., Walby, W.F., Mansoor, J.K., Chen, a T., 2001. Lung vagal afferent activity in rats with bleomycin-induced lung fibrosis. Respir. Physiol. 126, 9–27.
Sekizawa, S.I., Chen, C.Y., Bechtold, A.G., Tabor, J.M., Bric, J.M., Pinkerton, K.E., Joad, J.P., Bonham, A.C., 2008a. Extended secondhand tobacco smoke exposure induces plasticity in nucleus tractus solitarius second-order lung afferent neurons in young guinea pigs. Eur. J. Neurosci. 28, 771–781. https://doi.org/10.1111/j.1460-9568.2008.06378.x.
Sekizawa, S.I., Chen, C.Y., Bechtold, A.G., Tabor, J.M., Bric, J.M., Pinkerton, K.E., Joad, J.P., Bonham, A.C., 2008b. Extended secondhand tobacco smoke exposure induces plasticity in nucleus tractus solitarius second-order lung afferent neurons in young guinea pigs. Eur. J. Neurosci. 28, 771–781. https://doi.org/10.1111/j.1460-9568.2008.06378.x.
Smith, C., 1999. A persistent activity-dependent facilitation in chromaffin cells is caused by Ca2+ activation of protein kinase C. J. Neurosci. 19, 589–598.
Smith, C., Neher, E., 1997. Multiple forms of endocytosis in bovine adrenal chromaffin cells. J. Cell Biol. 139, 885–894.
Stincic, T.L., Frerking, M.E., 2015. Different AMPA receptor subtypes mediate the distinct kinetic components of a biphasic EPSC in hippocampal interneurons. Front. Synaptic Neurosci. 7. https://doi.org/10.3389/fnsyn.2015.00007.
Sulzer, D., Pothos, E.N., 2000. Regulation of quantal size by presynaptic mechanisms. Rev. Neurosci. 11, 159–212. https://doi.org/10.1515/REVNEURO.2000.11.2-3.159.
Takahashi, M., Kovalchuk, Y., Attwell, D., 1995. Pre- and postsynaptic determinants of EPSC waveform at cerebellar climbing fiber and parallel fiber to Purkinje cell synapses. J. Neurosci. 15, 5693–5702.
Travagli, R.A., Hermann, G.E., Browning, K.N., Rogers, R.C., 2006. Brainstem circuits regulating gastric function. Annu. Rev. Physiol. 68, 279–305. https://doi.org/10.1146/annurev.physiol.68.040504.094635.
Travagli, R.A., Hermann, G.E., Browning, K.N., Rogers, R.C., 2003. Musings on the wanderer: what's new in our understanding of vago-vagal reflexes? III. Activity-dependent plasticity in vago-vagal reflexes controlling the stomach. Am. J. Physiol. Gastrointest. Liver Physiol. 284, G180–G187. https://doi.org/10.1152/ajpgi.00413.2002.
Undem, B.J., 2005. The role of vagal afferent nerves in chronic obstructive pulmonary disease. Proc. Am. Thorac. Soc. https://doi.org/10.1513/pats.200504-033SR.
Vidruk, E.H., Olson Jr, E.B., Ling, L., Mitchell, G.S., 2001. Responses of single-unit carotid body chemoreceptors in adult rats. J Physiol (Lond). 531, 165–170. https://doi.org/10.1111/j.1469-7793.2001.0165j.x.
Ware, L., Matthay, M., 2000. The acute respiratory distress syndrome. N. Engl. J. Med. 342, 1334–1349. https://doi.org/10.1056/NEJM200005043421806.
Zhang, J., Malik, A., Choi, H.B., Ko, R.W.Y., Dissing-Olesen, L., MacVicar, B.A., 2014. Microglial {CR3} activation triggers long-term synaptic depression in the Hippocampus via {NADPH} oxidase. Neuron 82, 195–207. https://doi.org/10.1016/j.neuron.2014.01.043.
Zhang, W., Carreño, F.R., Cunningham, J.T., Mifflin, S.W., 2009. Chronic sustained hypoxia enhances both evoked EPSCs and norepinephrine inhibition of glutamatergic afferent inputs in the nucleus of the solitary tract. J. Neurosci. 29, 3093–3102. https://doi.org/10.1523/JNEUROSCI.2648-08.2009.
Zhang, W., Mifflin, S., 2010. Hypertension. Chronic hypertension enhances presynaptic inhibition by baclofen in the nucleus of the solitary tract, pp. 481–486. https://doi.org/10.1161/HYPERTENSIONAHA.109.145151.
Zhou, Q., Petersen, C.C., Nicoll, R.A., 2000. Effects of reduced vesicular filling on synaptic transmission in rat hippocampal neurones. J. Physiol. 525 (Pt 1), 195–206.
Zucker, R., Regehr, W., 2002. Short-term synaptic plasticity. Annu. Rev. Physiol. 64, 355–405. https://doi.org/10.1146/annurev.physiol.64.092501.114547.